HHS Public Access

Author manuscript

Microcirculation. Author manuscript; available in PMC 2016 July 01.

Published in final edited form as:

Microcirculation. 2015 July ; 22(5): 360–369. doi:10.1111/micc.12203.

Computational Network Model Prediction of Hemodynamic Alterations Due to Arteriolar Rarefaction and Estimation of Skeletal Muscle Perfusion in Peripheral Arterial Disease

Joshua L. Heuslein[1], **Xuanyue Li**[1], **Kelsey P. Murrell**[1], **Brian H. Annex**[1,2], **Shayn M. Peirce**[1], and **Richard J. Price**[1,3,4]

[1]Department of Biomedical Engineering, University of Virginia, Charlottesville, VA 22908

[2]Division of Cardiovascular Medicine, University of Virginia, Charlottesville, VA 22908

[3]Division of Radiology, University of Virginia, Charlottesville, VA 22908

[4]Division of Radiation Oncology, University of Virginia, Charlottesville, VA 22908

Abstract

Objective—To estimate the relative influence of input pressure and arteriole rarefaction on gastrocnemius muscle perfusion in patients with peripheral arterial disease (PAD) after exercise and/or percutaneous interventions.

Methods—A computational network model of the gastrocnemius muscle microcirculation was adapted to reflect rarefaction based on arteriolar density measurements from PAD patients, with and without exercise. A normalized input pressure was applied at the feeder artery to simulate both reduced and restored ankle-brachial index (ABI) in the PAD condition.

Results—In simulations of arteriolar rarefaction, resistance increased non-linearly with rarefaction, leading to a disproportionally large drop in perfusion. Additionally, perfusion was less sensitive to changes in input pressure as the degree of rarefaction increased. Reduced arteriolar density was observed in PAD patients and improved 33.8% after 3 months of exercise. In model simulations of PAD, ABI restoration yielded perfusion recovery to only 66% of baseline. When exercise training was simulated by reducing rarefaction, ABI restoration increased perfusion to 80% of baseline.

Conclusion—Microvascular resistance increases non-linearly with increasing arteriole rarefaction. Therefore, muscle perfusion becomes disproportionally less sensitive to ABI restoration as arteriole rarefaction increases. These results highlight the importance of restoring both microvascular structure and upstream input pressure in PAD therapy.

Keywords

rarefaction; microcirculation; network model; peripheral artery disease

Address for correspondence: Richard J. Price, University of Virginia, PO Box 800759, Health System, Charlottesville, VA 22908, USA. rjp2z@virginia.edu.

INTRODUCTION

Peripheral arterial disease (PAD) is caused by atherosclerotic plaque formation in the peripheral arteries, resulting in reduced blood flow to the lower extremities [3]. Approximately 12 million people are diagnosed with PAD in the United States alone [33]. As PAD prevalence increases with age (6% in individuals aged 50–60 years versus 10–20% aged >70 years) and both smoking and diabetes are causative factors, this number is likely to grow given our aging population and spread of the Western lifestyle worldwide [4,5,26,33].

There are two distinct clinical manifestations of PAD: critical limb ischemia (CLI) and intermittent claudication. Critical limb ischemia is the more severe form of PAD (11% of all PAD patients), wherein patients experience pain even at rest. Intermittent claudication is the more common form of PAD and is defined as calf or buttock pain with walking due to inadequate blood flow that is relieved with rest [3,32,33]. Currently, surgical and catheter-based revascularization approaches are used when patients have claudication that interferes with their lifestyle [48]. However, it has been shown that, while revascularization methods restore ankle-brachial index (ABI), which is defined as the ratio of the highest blood pressure in the posterior tibial or dosalis pedis artery to the highest blood pressure in the either brachial artery, many patients experience no significant improvement in tissue perfusion [3,49]. These findings suggest that PAD patients exhibit elevated hydraulic microvascular resistance in peripheral skeletal muscle that, in turn, impairs perfusion restoration, even when ABI is improved.

In support of this hypothesis, increased levels of skeletal muscle cell apoptosis and muscle atrophy in the gastrocnemius have been observed in patients with PAD [30]. Capillary density is reduced in this population as well, although it can be improved with supervised exercise [12]. While these results implicate the contribution of decreased capillary density to poor reperfusion, blood flow and nutrition supply in skeletal muscle are also governed by terminal arterioles upstream of the capillaries [43]. Importantly, terminal arteriole rarefaction (i.e. reduction in total number of arterioles) has been observed in arteriolar networks under pathological conditions, particularly in hypertensive animals [9,17,24,46]. We therefore hypothesized that the rarefaction of terminal arterioles in peripheral skeletal muscle also contributes substantially to the observed lack of perfusion restoration in response to surgical intervention.

To address this hypothesis and investigate the effects of arteriole input pressure and rarefaction on perfusion, we utilized a computational arteriolar network model based on morphological measurements of the rat gastrocnemius muscle microcirculation. In addition, we made pre-capillary arteriolar density measurements on biopsy specimens from human PAD patients. Skeletal muscle perfusion changes were then estimated by applying both relative arteriolar density and input pressure (set as proportional to ABI) changes from PAD patients to the model. The key result from this study is that microvascular resistance is predicted to increase non-linearly with increasing rarefaction. Because of this effect, muscle perfusion can become disproportionally less sensitive to ABI restoration as arteriole rarefaction increases.

MATERIALS AND METHODS

Computational Network Model Construction and Solution

A computational hemodynamic network model of an arteriole tree was constructed based on detailed morphological measurements of the gastrocnemius muscles of male Sprague-Dawley rats (final weight 441± 7g), as previously reported by Binder et al. and listed in Table 1 [8]. The branch order of the tree was assigned using a centrifugal system where a parent arteriole of order N gives rise to smaller diameter arterioles of order N+1. The number of arterioles per order was used to determine the number of nodes along each vessel. For a given order N, the total number of terminal nodes, or nodes that branch into two segments of lower order, was the total number of arterioles. The total number of intermediate nodes (i.e. nodes that branch into one segment of a lower order and one of the same order as the parent segment) was the total number of arterioles in the N+1 order minus twice the number of terminal nodes in the N order. These intermediate nodes were evenly distributed among vessel of the given order. Nodes were then numberd such that: (1) nodes in higher order vessels are indexed before those in a lower order vessel, and (2) intermediate nodes proceed any terminal nodes in vessels of the same order (Figure 1A).

The model solution was initiated by assigning input and output pressure boundary conditions. The pressure of all output nodes was assigned as 10mmHg to represent capillary pressure. Input pressure to the 2A feed arteriole was assigned as 80% of an assumed normal mean systemic pressure of 100mmHg. For the initial iteration of the model, the apparent viscosity (η) of each node-to-node segment was assigned as 4 cP and the discharge hematocrit (H_D) as 0.45 [8]. Arteriole segment conductance was computed assuming Poiseuille flow (Eq.1),

$$C=\frac{\pi D^4}{128\eta L} \quad (1)$$

where D is segment diameter and L is vessel segment length. Flow through a vessel segment bounded by nodes *i* and *j* (Q_{ij}) is described by

$$Q_{ij}=C_{ij}(P_i-P_j) \quad (2)$$

where P is the pressure at a given node and C is the conductance through the segment. As mass is conserved at each node, $\Sigma Q_i = 0$. A system of linear equations can therefore be generated into the matrix form:

$$\boldsymbol{CP}=\boldsymbol{Q} \quad (3)$$

Flow values were used to update H_D values using an empirically derived red blood cell distribution relationship (Eq 4) [37].

$$\begin{gathered} \text{logit}\,\phi = B\,\text{logit}\,\frac{\psi - X_0}{1-2X_0} + A \\ where\ \text{logit}\,x = \ln\frac{x}{1-x} \\ A = -6.96\ln\left(\frac{D_1}{D_2}\right)/D \\ B = 1 + \frac{6.98\,(1-H_D)}{D} \\ X_0 = \frac{0.4}{D} \end{gathered} \quad (4)$$

Here, φ is the red blood cell flux fraction entering one of the daughter branches, ψ is the flow fraction entering that branch, and D, D_1, D_2 are the diameters of the parent and two daughter branches. The resulting hematocrits are then used to calculate apparent viscosity in each arteriole segment using Eq.5 [37].

$$\begin{gathered} \eta = \left[1 + (\eta^* - 1)\frac{(1-H_D)^C - 1}{(1-0.45)^C - 1}\left(\frac{D}{D-1.1}\right)^2\right]\left(\frac{D}{D-1.1}\right)^2 \\ where\ \eta^* = 6e^{-0.085D} + 3.2 - 2.44e^{-.06D^{0.645}} \\ C = (0.8 + e^{-0.075D})\left(-1 + \frac{1}{1+10^{-11}D^{12}}\right) + \frac{1}{1+10^{-11}D^{12}} \end{gathered} \quad (5)$$

These new apparent viscosities were re-inserted into Eq. 3 to update flow in each arteriole segment. This process was repeated until the change in viscosity of a segment between consecutive iterations was within ≤ 0.02 cP [8].

Vessel Rarefaction in an Individual Tree

Vessel segments of a given order were removed from the tree at random to simulate a given degree of rarefaction (Figure 1A–C). The vessel that underwent rarefaction and all vessels downstream were then assigned a conductance of 0.01. This value was chosen to ensure the segments that experienced rarefaction had effectively no flow. If two vessels that underwent rarefaction originated from the same higher order parent vessel, the parent vessel also underwent rarefaction. Input pressure to the 2A arteriole was set to 80mmHg, 80% of systemic pressure, and vessels that experienced rarefaction were excluded from hematocrit correction.

Whole Muscle Perfusion

A total of 8 individual trees were placed equidistant along a main feeder artery to simulate the entire arteriolar network of the gastrocnemius. For each individual tree placed equidistant along a main feeder artery, vessels of a given order in that individual tree were removed at random to simulate the given degree of rarefaction as described above. Conductance was calculated as the quotient of total flow and pressure change across the individual arteriole tree. This was repeated for each individual arteriole tree along the main feeder artery (Figure 1D). To obtain the flow in each segment of the main feeder artery and to calculate total muscle perfusion, each individual tree along the main feeder artery was assigned the previously calculated conductance and mass conservation was applied at each node. The main feeder artery input pressure was assumed to be 80mmHg and was normalized by a scaling factor ranging from 1.0 – 0.5 to determine influence of input pressure on total perfusion. Main feed artery output pressure was assigned as 2mmHg less than the input pressure and transverse arteriole output pressure as capillary pressure

(10mmHg) [8]. The conductance of the feed artery was calculated assuming Poiseuille flow and vessel diameter of 240μm and an estimated length of 3cm based on measurements from a previous study on Sprague-Dawley rats of a similar size [11].

Exercise Training and Immunohistological Analysis

Research protocols in this study were approved by the institutional review boards at Duke University and the University of Colorado. Patient selection, exercise training, biopsy collection, and immunohistological analysis were performed as previously published [12]. Briefly, PAD subjects had symptom-limiting intermittent claudication and an ABI <0.90 at rest or a 20% decrease in ABI after exercise, or angiographic evidence of PAD. PAD subjects performed supervised exercise three times per week until 36 sessions were complete. Exercise consisted of walking on a treadmill at the workload at which claudication onset was documented with rest given as necessary. Exercise and rest cycles were repeated during each training session until an accumulation of 30–40 minutes of active walking was completed. Skeletal muscle biopsies (20–40mg) were taken from the medial aspect of the gastrocnemius at 0, 3, and 12 weeks. These biopsies were sectioned and stained with a mouse anti-human CD31 antibody (clone 9G11, 20μg/mL, R&D systems, Inc) followed by goat anti-mouse Alexa Fluor 488 conjugated secondary antibody (40μg/mL). Two fields of view were imaged at a final magnification of 100x on a Zeiss LSM 510-UV confocal microscope. Arteriolar density was determined as the number of non-capillary (>5μm diameter) $CD31^+$ vessels per mm^2 of tissue by a trained blinded observer. Only PAD patients that completed the exercise protocol and provided biopsies at 0, 3, and 12 weeks were included in our analysis (n=18).

Statistical Analysis

A one way ANOVA followed by post-hoc testing using the Bonferroni correction for multiple comparisons was performed for arteriolar density measurements in PAD patients with supervised exercise and for simulations of PAD conditions. Probability values of <0.05 were considered significant for all tests.

RESULTS

Arteriole rarefaction in simulated individual arteriole tree

To investigate how rarefaction of different caliber vessels affects perfusion, we simulated ~10–80% random rarefaction of arterioles in both 4A and 7A order vessels in our computational model of an arteriole tree with input pressure of 80mmHg (Figure 1A–C). These two vessel orders were chosen to compare resistance arteries (4A), which are known to have a large influence on microvascular network resistance [15] and intraluminal pressure drop across the network[8], to pre-capillary vessels (7A) that do not [8]. Not unexpectedly, across the entire range of simulated rarefaction, the rarefaction of 4A arterioles decreased total arteriolar density (Figure 2A) and total relative perfusion (Figure 2B) to a greater extent than a similar degree of rarefaction in 7A arterioles. Furthermore, for both the 4A and 7A rarefaction simulations, the curves became steeper (i.e. greater negative slope) with increasing vessel drop-out, such that increasing the level of rarefaction led to a disproportionally large increase in resistance and drop in perfusion.

In contrast to 7A rarefaction, the removal of one 4A vessel could lead to the dropout of an entire portion of the arteriole tree due to the additional removal of all its daughter vessels resulting in large, avascular areas along the tree. Furthermore, relative dispersion measurements of I^{125}-labeled albumin washout experiments support an increase in perfusion spatial heterogeneity throughout the gastrocnemius microvasculature in an experimental model of peripheral vascular disease [13]. In individual arteriolar tree simulations, 4A rarefaction leads to an increase in flow heterogeneity as measured by the coefficient of variation of total perfusion compared to a similar degree of 7A rarefaction (Figure S1). Finally, in our model, an extremely high degree of 7A rarefaction (~70%) would be required to obtain a 50% reduction in arteriolar density from baseline whereas only ~50% of 4A arterioles would need to undergo rarefaction to obtain the same arteriolar density. Since rarefaction of 4A vessels is able to better simulate the large avascular regions observed in clinical and experimental models of PAD as well as the perfusion heterogeneity observed in an experimental model of PAD, this mode of rarefaction was use for all subsequent simulations.

Whole muscle perfusion in simulated PAD

We next sought to investigate the effect of 4A rarefaction on whole muscle perfusion in PAD. A normalized input pressure to the feed artery was used to simulate the ankle-brachial index (ABI) range in human PAD patients, with the assumption that the input pressure in our model scales proportionally with ABI. Total relative perfusion was calculated for six levels of 4A rarefaction (0%, 22%, 33%, 44%, 55%, and 77%) across a range of normalized input pressures (Figure 3). As expected, a decrease in normalized input pressure or increase in rarefaction resulted in decreased muscle perfusion. Interestingly, as the degree of rarefaction increased, total gastrocnemius perfusion was less sensitive to changes in normalized input pressure. This phenomenon is evident in the reduced slope seen with increasing rarefaction in Figure 3. As the slope is proportional to the conductance of the microvascular tree, the diminished response to upstream revascularization is directly related to the reduced conductance caused by rarefaction.

Microvascular Rarefaction and Perfusion Estimation in Human PAD Patients

Arteriolar (>5 μm diameter) density for human gastrocnemius biopsies for healthy patients, PAD patients, and PAD patients after either three weeks or twelve weeks of regular, supervised exercise are presented in Figure 4. Only PAD patients that completed the exercise protocol and provided biopsies at each time-point were included in our analysis (n=18). In normal, healthy patients approximately 30 arterioles were counted in each field of view. PAD patients exhibited a significant decrease in baseline arteriolar density (54.2 ± 0.07% of normal patients). Patients with PAD that performed regular supervised exercise for three months showed an increase in arteriolar density (33.75% increase) compared to PAD patients without exercise, although this was not statistically significant ($p = 0.283$). While exercise tended to improve arteriolar density in PAD patients, it was only able to restore up to 72.5 ± 0.11% of that in healthy patients. These data imply that patients with PAD experience microvascular rarefaction and that exercise decreases the extent of this rarefaction, though only partially, as a significant deficit in microvascular density remains despite exercise.

We then simulated the effects of PAD, both with and without the therapeutic options of exercise and/or percutaneous intervention, on gastrocnemius perfusion in our computational model. In our baseline PAD simulations, 44% of 4A arterioles underwent rarefaction to reflect a similar reduction in arteriolar density (56% of baseline, Fig. 2A & Fig. 4) as measured in human PAD patient biopsies. Exercise was then simulated by decreasing the fraction of 4A arterioles experiencing rarefaction to 22% to reflect the increase in arteriolar density (78% of baseline, Fig. 2A & Fig. 4) in PAD patients after 3 months of supervised exercise. Exercise alone modestly increased total perfusion from 40.35 ± 0.01 to 48.77 ± 0.02% from baseline in simulated PAD conditions (Figure 5).

While exercise can reduce the degree of rarefaction in PAD patients, lower extremity bypass surgery has been demonstrated to improve ABI to near normal levels [14,49]. For our model, an increase of normalized input pressure from 0.6 to 0.9 was used to simulate percutaneous interventions based on a recent study wherein 10 PAD patients demonstrated an increase in resting ABI from 0.62 ± 0.17 to 0.93 ± 0.25 10-months after lower extremity percutaneous intervention [51]. Our model estimates that as the degree of vessel rarefaction increases, restoring ABI results in a progressively smaller restoration of perfusion (Figure 3). We therefore simulated a percutaneous intervention to restore ABI both with and without a simultaneous reduction in arteriolar rarefaction (44% to 22%) to mimic exercise training. Consistent with our prediction, we observe that increasing ABI from 0.6 to 0.9 improved total perfusion to 66.52 ± 0.02% of baseline in patients with 44% rarefaction alone. However total perfusion was restored to 80.04 ± 0.03% of baseline when ABI was increased from 0.6 to 0.9 and the degree of arteriolar rarefaction was simultaneously reduced to mimic the effects of exercise (Figure 5).

DISCUSSION

The objectives of this study were (i) to develop and implement a computational network model capable of determining the effects of arteriole rarefaction and arteriole input pressure on gastrocnemius perfusion and (ii) to use this model to predict how supervised exercise and/or percutaneous interventions will affect perfusion in PAD patients exhibiting reduced peripheral skeletal muscle arteriolar density. To achieve these objectives, we constructed a computational arteriolar network model based on previously published morphological measurements of the rat gastrocnemius muscle. Similar modeling approaches have been used to study microvascular remodeling [8,15,16,22,34–36,38,39] and the influence of capillary rarefaction [15] on hemodynamics. By removing different fractions of 4^{th} and 7^{th} order arterioles in a spatially randomized manner and calculating total network flow, we determined that perfusion decreases non-linearly with increasing rarefaction. Next, the model was adapted to simulate baseline PAD conditions and perfusion changes in PAD resulting from exercise and/or percutaneous interventions by adjusting arteriole density and input pressure based on measured values. The pivotal prediction from this model is that, as the level of microvascular rarefaction increases, peripheral skeletal muscle perfusion becomes considerably less sensitive to input pressure restoration. Thus, the computational model recapitulates a key element of clinical PAD studies of patients with intermittent claudication, wherein perfusion restoration was not proportional to ABI restoration within

subjects with claudication [49], and suggests that these clinical results may be due to a non-linear relationship between microvascular rarefaction and hydraulic resistance.

Computational Models of Microvascular Remodeling and Resistance

Computational network models have been used extensively in the past to examine how changes in microvascular network structure affect whole-network hemodynamics [6,8,47,15,16,22,34–36,38,39]. Indeed, we used an earlier version of the gastrocnemius muscle computational model to accurately predict flow increases due to arteriolar remodeling in response to exercise training [8]. Our current model applies the relative changes in human arteriolar densities observed in PAD patients to a model of the rat gastrocnemius to predict the influence of PAD, exercise, and percutaneous interventions on perfusion. We used data from rat specimens to construct the model because no whole mount or three-dimensional anatomical data detailing the microvascular morphology of the human gastrocnemius currently exists. Indeed, imaging techniques such as magnetic resonance angiography (MRA) and computed tomography angiography (CTA) do not have the spatial resolution necessary to reveal microvascular structure at the level of the terminal arterioles, which lie immediately upstream of the capillaries. Nonetheless, despite being based on data from rat microcirculation, the model was fully capable of predicting relative changes in muscle perfusion, which we believe is still useful for understanding the fundamental relationship between rarefaction and network perfusion in PAD and to generating hypotheses to guide future experiments regardless of species.

Another potential limitation of this study is the application of data from cross-sectioned specimens to a network model. Similar histological analyses of cross-sectioned human gastrocnemius muscle biopsies have been used previously to draw conclusions about capillary density [12,42], muscle fiber morphology [40], and apoptosis [30] in patients with PAD. However, we also acknowledge that biopsy specimens may not fully capture spatial heterogeneities in rarefaction that may occur in patients with PAD. Moreover, potential differences in the morphological properties of the vasculature in patients with PAD, such as branching patterns, vessel diameter, vessel reactivity, and muscle metabolism were not incorporated into our model, though each may affect muscle perfusion. The contributions of each factor could be assessed in future iterations of our model as imaging methods continue to improve toward enabling the non-invasive, three-dimensional analysis of the human microvasculature and as we continue to better understand the pathophysiology of PAD.

The current iteration of our model showed that 4A rarefaction yielded greater resistance changes than 7A rarefaction. This result was not only intuitive and expected, but also supported by a previous study showing the larger arteriole rarefaction elicits a greater impact on resistance increase [15]. The model also predicted that, as arteriolar rarefaction increases, microvascular resistance will increase non-linearly. This relationship between rarefaction and resistance was also not unexpected as previous computational modeling studies have shown similar results. For example, total perfused capillary surface area begins to decrease rapidly when ~70% of capillary entrances are blocked [6], and a similar type of relationship exists between resistance and the fraction of capillaries that are obstructed due to leukocyte plugging [47].

In contrast to our results, a previous study aimed at determining the influence of arteriole network changes in hamster cheek pouch on total peripheral resistance yielded smaller resistance increases for similar degrees of rarefaction [15]. Moreover, resistance did not increase exponentially as rarefaction increased [15]. One possible explanation for these differences could stem from morphological and topological differences between the networks. Additionally, 4A rarefaction was not extended over the same range used in our study, and it is possible that similar relationships would be observed with their model at higher rarefaction levels. The current model also uses a set arrangement of vessels in each order. It has been shown that variation in the placement of the vessels can cause variation in the predicted value [8,15].

Predicted Influence of PAD, Exercise, and/or Percutaneous Interventions on Perfusion

To our knowledge, this computational network model is the first to provide estimates of relative perfusion as a function of input pressure and arteriolar density in PAD. We ultimately chose to use 4A rarefaction in our perfusion estimates as it also resulted in the dropout of all smaller downstream arterioles and therefore better simulated clinical and experimental models of PAD in which there is heterogeneous perfusion [13] and large avascular, necrotic regions within the gastrocnemius [18,27]. Exercise is recommended for PAD patients [1] and has been shown to improve arteriolar density, capillary density [42], perfusion [12,19], and patient functional outcomes [19,20]. Additionally, we show a trend of increased arteriolar density after 3 months of supervised exercise in PAD patients with intermittent claudication and was simulated in our model by choosing a 4A rarefaction level that approximated arteriolar density as measured in biopsies of these patients. Percutaneous interventions were simulated by increasing input pressure in proportion to clinical ABI measurements. Due to the non-linear relationship between rarefaction and microvascular resistance in the arteriole tress, ABI restoration led to disproportionally lower perfusion at higher rarefaction levels. These results are consistent with the lack of observed perfusion improvement in PAD patients with intermittent claudication that underwent vascular surgery to restore ABI from 0.6 to 0.9 [49]. When we simulate the effects of exercise by reducing rarefaction, ABI restoration increases perfusion to a greater extent. Thus, our results predict that revascularization may be more effective in restoring perfusion when arteriolar rarefaction is also reduced in PAD patients. To our knowledge, only one clinical study has investigated the combination of exercise and/or revascularization on perfusion in PAD patients with intermittent claudication. In this study, the addition of training to surgery created a trend of improved maximal calf blood flow, though these results were not statistically significant [25].

Our results may also have bearing on the interpretation of clinical trials to restore upstream perfusion pressure via revascularization or to therapeutically stimulate angiogenesis [10,21,23,28,40,41,44,45]. Stenting of the iliac artery has been shown to have no measureable effect on gastrocnemius muscle perfusion in humans [49]. Moreover, the results of the CLEVER trial demonstrated that supervised exercise improved peak treadmill walking time to a greater extent than stent revascularization in PAD patients with claudication, highlighting the need to restore the underlying microvasculature to improve patient outcome [31]. Indeed, both our model predictions and a recent experimental study

using myoglobin transgenic mice suggest the need to restore microvascular structure [29]. Our data support the hypothesis that a combination of microvascular expansion via exercise and stenting of a large vessel would be an “optimal” treatment, though that clinical study has not yet been definitively completed. However, if given a choice between revascularization of a large vessel versus microvascular expansion of terminal arterioles and capillaries via exercise, the latter would be predicted to have a greater effect on muscle perfusion and on improving clinical outcomes in PAD patients with intermittent claudication.

Moreover, it is also important to emphasize that, while arteriogenesis and angiogenesis can markedly expand microvascular networks and increase perfusion, tissue clearance and metabolism may also contribute toward the recovery from vascular occlusions [27]. In PAD patients, while metabolism, muscle perfusion, and stenosis severity correlate with functional outcomes, there is an uncoupling of calf muscle perfusion and metabolism [2]. In addition, peak walking time in PAD patients with intermittent claudication subjected to 12 weeks of exercise training correlates with a decrease in plasma short-chain acylcarnitine concentration, which reflects the metabolic state of the muscle, but does not correlate to perfusion [19]. In all, these studies highlight the need for future studies investigating the interactions of arteriogenesis, angiogenesis, and tissue clearance and metabolism. Future strategies utilizing concomitant targeting of upstream pressure restoration via arteriogenesis or percutaneous intervention, microvascular function, and muscle repair may prove a more effective therapeutic approach for patients suffering from PAD.

Supplementary Material

Refer to Web version on PubMed Central for supplementary material.

Acknowledgments

Supported by AHA 13GRNT16910073, NIH R01 HL101200, NIH R01 HL 075752, NIH R01 HL121635 and NSF DGE 1315231

References

1. Anderson JL, Halperin JL, Albert NM, Bozkurt B, Brindis RG, Curtis LH, DeMets D, Guyton RA, Hochman JS, Kovacs RJ, Ohman EM, Pressler SJ, Sellke FW, Shen W-K. Management of patients with peripheral artery disease (compilation of 2005 and 2011 accf/aha guideline recommendations) a report of the american college of cardiology foundation/american heart association task force on practice guidelines. Circulation. 2013; 127:1425–1443. [PubMed: 23457117]
2. Anderson JD, Epstein FH, Meyer CH, Hagspiel KD, Wang H, Berr SS, Harthun NL, Weltman A, Dimaria JM, West AM, Kramer CM. Mutltifactorial determinants of functional capacity in peripheral arterial disease: uncoupling of calf muscle perfusion and metabolism. J Am Coll Cardiol. 2009; 54:628–635. [PubMed: 19660694]
3. Annex BH. Therapeutic angiogenesis for critical limb ischaemia. Nat Rev Cardiol. 2013; 10:387–96. [PubMed: 23670612]
4. Beckman JA, Creager MA, Libby P. Diabetes and atherosclerosis: epidemiology, pathophysiology, and management. JAMA. 2002; 287:2570–2581. [PubMed: 12020339]
5. Belch JJF, Topol EJ, Agnelli G, Bertrand M, Califf RM, Clement DL, Creager Ma, Easton JD, Gavin JR, Greenland P, Hankey G, Hanrath P, Hirsch AT, Meyer J, Smith SC, Sullivan F, Weber Ma. Critical issues in peripheral arterial disease detection and management: a call to action. Arch Intern Med. 2003; 163:884–92. [PubMed: 12719196]

6. Benedict KF, Coffin GS, Barrett EJ, Skalak TC. Hemodynamic systems analysis of capillary network remodeling during the progression of type 2 diabetes. Microcirculation. 2010; 18:63–73. [PubMed: 21166927]
7. Berceli SA, Hevelone ND, Lipsitz SR, Bandyk DF, Clowes AW, Moneta GL, Conte MS. Surgical and endovascular revision of infrainguinal vein bypass grafts: analysis of midterm outcomes from the prevent iii trial. J Vasc Surg. 2007; 46:1173–1179. [PubMed: 17950564]
8. Binder KW, Murfee WL, Song J, Laughlin MH, Price RJ. Computational network model prediction of hemodynamic alterations due to arteriolar remodeling in interval sprint trained skeletal muscle. Microcirculation. 2007; 14:181–192. [PubMed: 17454671]
9. Chen IH, Prewitt RL, Dowell RF. Microvascular hypertensive rarefaction in spontaneously rat cremaster muscle. Am J Physiol Hear Circ Physiol. 1981; 241:306–310.
10. Creager MA, Olin JW, Belch JJF, Moneta GL, Henry TD, Rajagopalan S, Annex BH, Hiatt WR. Effect of hypoxia-inducible factor-1α gene therapy on walking performance in patients with intermittent claudication. Circulation. 2011; 124:1765–1773. [PubMed: 21947297]
11. Delp MD, Colleran PN, Wilkerson MK, McCurdy MR, Muller-Delp J. Structural and functional remodeling of skeletal muscle microvasculature is induced by simulated microgravity. Am J Physiol Hear Circ Physiol. 2000; 278:H1866–H1873.
12. Duscha BD, Robbins JL, Jones WS, Kraus WE, Lye RJ, Sanders JM, Allen JD, Regensteiner JG, Hiatt WR, Annex BH. Angiogenesis in skeletal muscle precede improvements in peak oxygen uptake in peripheral artery disease patients. Arterioscler Thromb Vasc Biol. 2011; 31:2742–8. [PubMed: 21868709]
13. Frisbee JC, Wu F, Goodwill AG, Butcher JT, Beard DA. Spatial heterogeneity in skeletal muscle microvascular blood flow distribution is increased in the metabolic syndrome. Am J Physiol Regul Integr Comp Physiol. 2011; 301:R975–986. [PubMed: 21775645]
14. Gardner AW, Killewich LA. Lack of functional benefits following infrainguinal bypass in peripheral arterial occlusive disease patients. Vasc Med. 2001; 6:9–14. [PubMed: 11358164]
15. Greene AS, Tonellato PJ, Lui J, Lombard JH, Cowley AW. Microvascular rarefaction and tissue vascular resistance in hypertension. Am J Physiol Hear Circ Physiol. 1989; 256:H126–H131.
16. Gruionu G, Hoying JB, Pries AR, Secomb TW. Structural remodeling of mouse gracilis artery after chronic alteration in blood supply. Am J Physiol Hear Circ Physiol. 2005; 288:2047–2054.
17. Harper RN, Moore MA, Marr MC, Watts LE, Hutchins PM. Arteriolar rarefaction in the conjunctiva of human essential hypertensives. Microvasc Res. 1978; 16:369–372. [PubMed: 748720]
18. Hedberg B, Angquist K-A, Henriksson-Larsen K, Sjöström M. Fibre loss and distibution in skeletal muscle from patients with severe peripheral arterial insufficiency. Eur J Vasc Surg. 1989; 3:315–322. [PubMed: 2767254]
19. Hiatt WR, Regensteiner JG, Hargarten ME, Wolfel EE, Brass EP. Benefit of exercise conditioning for patients with peripheral arterial disease. Circulation. 1990; 81:602–609. [PubMed: 2404633]
20. Hiatt WR, Wolfel EE, Meier RH, Regensteiner JG. Superiority of treadmill walking exercise versus strength training for patients with peripheral arterial disease: implications for the mechanism of the training response. Circulation. 1994; 90:1866–1874. [PubMed: 7923674]
21. Kastrup J, Jørgensen E, Rück A, Tägil K, Glogar D, Ruzyllo W, Bøtker HE, Dudek D, Drvota V, Hesse B, Thuesen L, Blomberg P, Gyöngyösi M, Sylvén C. Direct intramyocardial plasmid vascular endothelial growth factor-a165 gene therapy in patients with stable severe angina pectoris a randomized double-blind placebo-controlled study: the euroinject one trial. J Am Coll Cardiol. 2005; 45:982–8. [PubMed: 15808751]
22. Kiani MF, Pries AR, Hsu LL, Sarelius IH, Cokelet GR. Fluctuations in microvascular blood flow parameters caused by hemodynamic mechanisms. Am J Physiol Hear Circ Physiol. 1994; 266:H1822–H1828.
23. Kusumanto YH, van Weel V, Mulder NH, Smit AJ, van den Dungen JJAM, Hooymans JMM, Sluiter WJ, Tio RA, Quax PHA, Gans ROB, Dullaart RPF, Hospers GAP. Treatment with intramuscular vascular endothelial growth factor gene compared with placebo for patients with diabetes mellitus and critical limb ischemia: a double-blind randomized trial. Hum Gene Ther. 2006; 17:683–91. [PubMed: 16776576]

24. Lombard JH, Hinojosa-Laborde C, Cowley AW. Hemodynamics and microcirculatory alterations in reduced renal mass hypertension. Hypertension. 1989; 13:128–138. [PubMed: 2914735]
25. Lundgren F, Dahllof A-G, Lundholm K, Scherstén T, Volkmann R. Intermittent claudication-surgical reconstruction or physical training ? Ann Surg. 1989; 209:346–355. [PubMed: 2647051]
26. Marso SP, Hiatt WR. Peripheral arterial disease in patients with diabetes. J Am Coll Cardiol. 2006; 47:921–9. [PubMed: 16516072]
27. Meisner JK, Annex BH, Price RJ. Despite normal arteriogenic and angiogenic responses, hind limb perfusion recovery and necrotic and fibroadipose tissue clearance are impaired in matrix metalloproteinase 9-deficient mice. J Vasc Surg. 201410.1016/j.jvs.2014.01.038
28. Meisner JK, Price RJ. Spatial and temporal coordination of bone marrow-derived cell activity during arteriogenesis: regulation of the endogenous response and therapeutic implications. Microcirculation. 2010; 17:583–599. [PubMed: 21044213]
29. Meisner JK, Song J, Annex BH, Price RJ. Myoglobin overexpression inhibits reperfusion in the ischemic mouse hindlimb through impaired angiogenesis but not arteriogenesis. Am J Pathol. 2013; 183:1–10.
30. Mitchell RG, Duscha BD, Robbins JL, Redfern SI, Chung J, Bensimhon DR, Kraus WE, Hiatt WR, Regensteiner JG, Annex BH. Increased levels of apoptosis in gastrocnemius skeletal muscle in patients with peripheral arterial disease. Vasc Med. 2007; 12:285–290. [PubMed: 18048464]
31. Murphy TP, Cutlip DE, Regensteiner JG, Mohler ER, Cohen DJ, Reynolds MR, Massaro JM, Lewis Ba, Cerezo J, Oldenburg NC, Thum CC, Goldberg S, Jaff MR, Steffes MW, Comerota AJ, Ehrman J, Treat-Jacobson D, Walsh ME, Collins T, et al. Supervised exercise versus primary stenting for claudication resulting from aortoiliac peripheral artery disease: six-month outcomes from the claudication: exercise versus endoluminal revascularization (clever) study. Circulation. 2012; 125:130–9. [PubMed: 22090168]
32. Nehler MR, Duval S, Diao L, Annex BH, Hiatt WR, Rogers K, Zakharyan A, Hirsch AT. Epidemiology of peripheral arterial disease and critical limb ischemia in an insured national population. J Vasc Surg. 2014:1–10.10.1016/j.jvs.2014.03.290
33. Norgren L, Hiatt WR, Dormandy Ja, Nehler MR, Harris KA, Fowkes FGR. Inter-society consensus for the management of peripheral arterial disease (tasc ii). Eur J Vasc Endovasc Surg. 2007; 33:S1–S75. [PubMed: 17140820]
34. Price RJ, Skalak TC. Circumferential wall stress as a mechanism for arteriolar rarefaction and proliferation in a network model. Microvasc Res. 1994; 47:188–202. [PubMed: 8022319]
35. Price RJ, Less JR, Van Gieson EJ, Skalak TC. Hemodynamic stresses and structural remodeling of anastomosing arteriolar networks: design principles of collateral arterioles. Microcirculation. 2002; 9:111–24. [PubMed: 11932778]
36. Price RJ, Skalak TC. A circumferential stress-growth rule predicts arcade arteriole formation in a network model. Microcirculation. 1995; 2:41–51. [PubMed: 8542539]
37. Pries AR, Secomb TW, Gessner T, Sperandio MB, Gross JF, Gaehtgens P. Resistance to blood flow in microvessels in vivo. Circ Res. 1994; 75:904–915. [PubMed: 7923637]
38. Pries AR, Reglin B, Secomb TW. Remodeling of blood vessels: responses of diameter and wall thickness to hemodynamic and metabolic stimuli. Hypertension. 2005; 46:725–31. [PubMed: 16172421]
39. Pries AR, Secomb TW, Gaehtgens P. Design principles of vascular beds. Circ Res. 1995; 77:1017–1023. [PubMed: 7554136]
40. Rajagopalan S, Mohler ER, Lederman RJ, Mendelsohn FO, Saucedo JF, Goldman CK, Blebea J, Macko J, Kessler PD, Rasmussen HS, Annex BH. Regional angiogenesis with vascular endothelial growth factor in peripheral arterial disease a phase ii randomized, double-blind, controlled study of adenoviral delivery of vascular endothelial growth factor 121 in patients with disabling intermittent cla. Circulation. 2003; 108:1933–1938. [PubMed: 14504183]
41. Ripa RS, Jørgensen E, Wang Y, Thune JJ, Nilsson JC, Søndergaard L, Johnsen HE, Køber L, Grande P, Kastrup J. Stem cell mobilization induced by subcutaneous granulocyte-colony stimulating factor to improve cardiac regeneration after acute st-elevation myocardial infarction: result of the double-blind, randomized, placebo-controlled stem cells in myocardial infarc. Circulation. 2006; 113:1983–92. [PubMed: 16531621]

42. Robbins JL, Jones WS, Duscha BD, Allen JD, Kraus WE, Regensteiner JG, Hiatt WR, Annex BH. Relationship between leg muscle capillary density and peak hyperemic blood flow with endurance capacity in peripheral artery disease. J Appl Physiol. 2011; 111:81–86. [PubMed: 21512146]
43. Sarelius IH. Cell flow path influences transit time through striated muscle capillaries. Am J Physiol Hear Circ Physiol. 1986; 250:H899–H907.
44. Simons M. Pharmacological treatment of coronary artery disease with recombinant fibroblast growth factor-2: double-blind, randomized, controlled clinical trial. Circulation. 2002; 105:788–793. [PubMed: 11854116]
45. Subramaniyam V, Waller EK, Murrow JR, Manatunga A, Lonial S, Kasirajan K, Sutcliffe D, Harris W, Taylor WR, Alexander RW, Quyyumi Aa. Bone marrow mobilization with granulocyte macrophage colony-stimulating factor improves endothelial dysfunction and exercise capacity in patients with peripheral arterial disease. Am Hear J. 2009; 158:53–60.
46. Sullivan JM, Prewitt RL, Josephs JA. Attenuation of the microcirculation in young patients with high-output borderline hypertension. Hypertension. 1983; 5:844–851. [PubMed: 6654450]
47. Warnke KC, Skalak TC. The effects of leukocytes on blood flow in a model skeletal muscle capillary network. Microvasc Res. 1990; 40:118–36. [PubMed: 2398826]
48. Weinber MD, Lau JF, Rosenfield K, Olin JW. Peripheral artery disease. Part 2: medical and endovascular treatment. Nat Rev Cardiol. 2011; 8:429–441. [PubMed: 21670746]
49. West AM, Anderson JD, Epstein FH, Meyer CH, Hagspiel KD, Berr SS, Harthun NL, Weltman AL, Annex BH, Kramer CM. Percutaneous intervention in peripheral artery disease improves calf muscle phosphocreatine recovery kinetics : a pilot study. Vasc Med. 2012; 17:3–9. [PubMed: 22363013]

Perspectives

- A computational arteriolar network model was generated based on morphological measurements of the rat gastrocnemius muscle to investigate the effects of arteriole input pressure and rarefaction on the gastrocnemius perfusion response and to estimate perfusion in PAD patients after exercise and/or percutaneous interventions using human arteriolar density measurements.
- Human PAD patients undergo significant arteriolar rarefaction and are less responsive to a restoration in ABI as degree of rarefaction increases.
- These results emphasize the importance of designing therapeutics to restore normal microvascular structure and function in combination with surgical revascularization in patients with PAD.

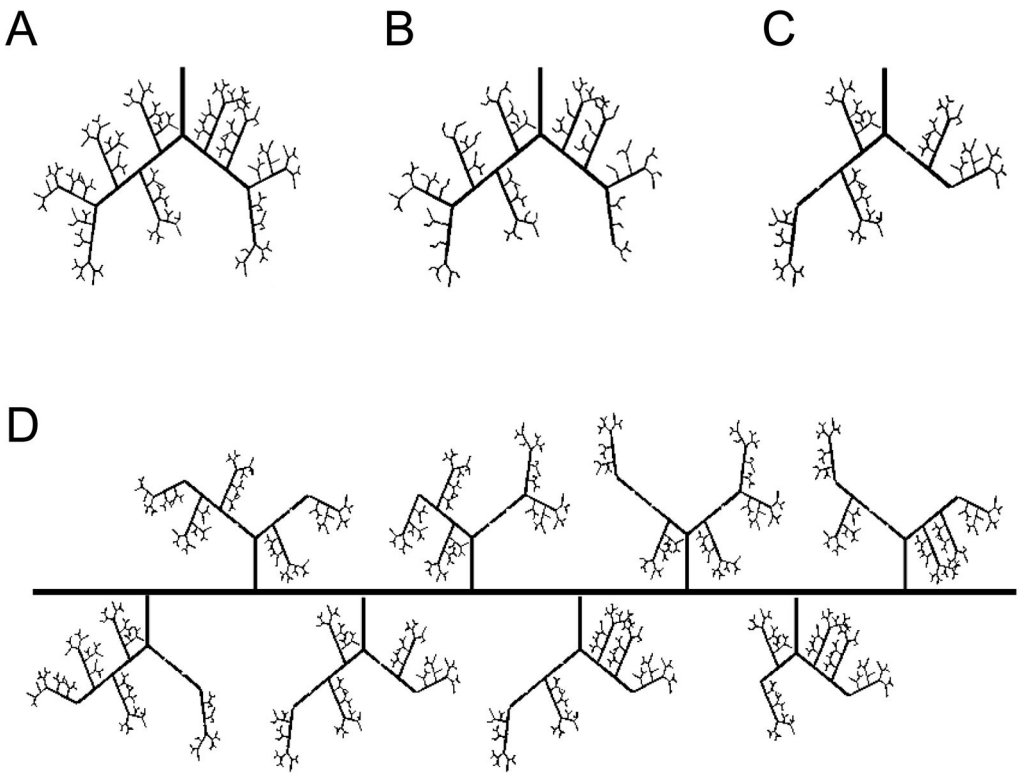

Figure 1. Schematic of arteriolar network generation

Vessel rarefaction in individual arteriole trees with (A) 0%, (B) 44% rarefaction of 7A vessels, (C) and 44% rarefaction of 4A vessels. (D) In whole muscle perfusion simulations, individual arteriole trees with a given degree of random rarefaction (44% of 4A vessels here) were placed equidistant along a main feeder artery. Total conductance was calculated for each individual arteriole tree.

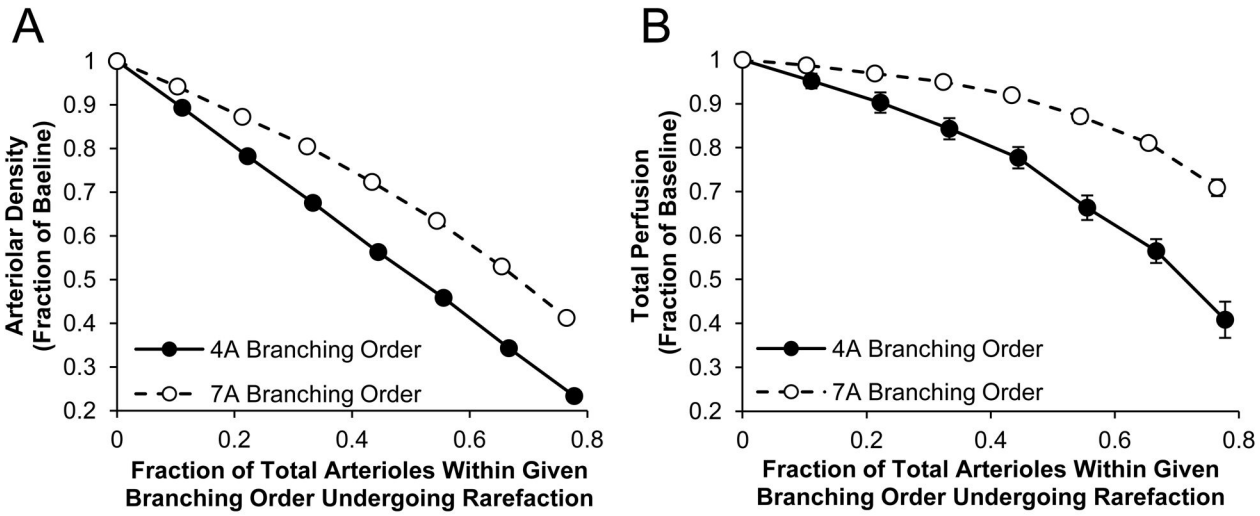

Figure 2. Increasing degree of rarefaction leads to a disproportionally large drop in perfusion

A computational network model of an arteriole tree with a constant input pressure was constructed based on the measurements listed in Table 1. Rarefaction was simulated by randomly selecting arterioles of a given order and setting the conductance and all corresponding downstream vessel conductance to 0.01. Percentage of arterial tree remaining (A) and total relative perfusion (B) were calculated for ~10% through ~80% rarefaction in both 4A and 7A branching order arterioles (n=10). Data are mean ± standard deviation.

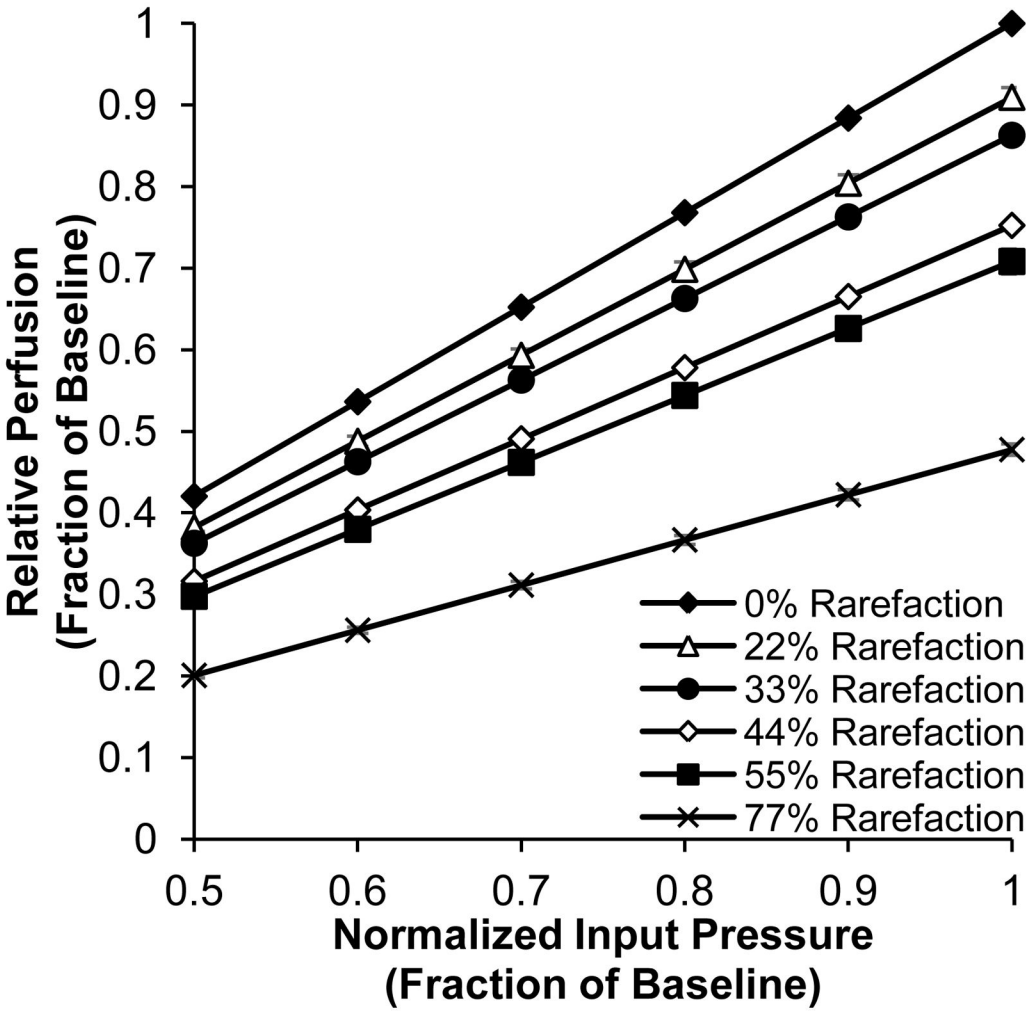

Figure 3. Muscle perfusion restoration is less sensitive to input pressure increases at high rarefaction levels

Total mean perfusion relative to baseline (0% rarefaction and 1.0 normalized input pressure) calculated for normalized input pressures ranging from 0.5 – 1.0 with 0%, 22%, 33%, 44%, 55%, and 77% rarefaction of 4A arterioles (n=10). Data are mean ± standard deviation.

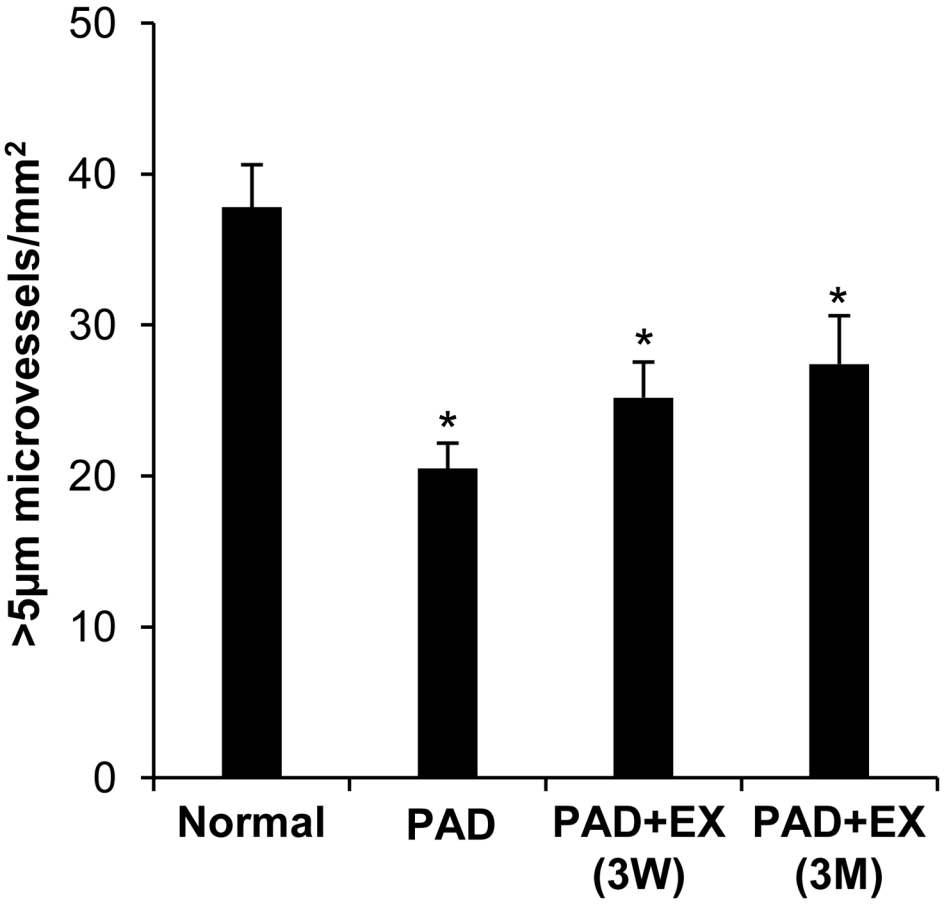

Figure 4. Reduced arteriolar density in human PAD patients

Arteriolar density was analyzed from human gastrocnemius muscle biopsies in healthy subjects (normal, n = 33) and subjects with PAD (n = 18) at baseline (PAD), after 3 weeks (3W), and after 3 months (3M) of regular supervised exercise (EX). Arteriolar density was determined as the number of non-capillary (>5µm diameter) $CD31^+$ vessels per mm^2 of tissue. Data are mean ± SEM. *$p < 0.05$ versus normal.

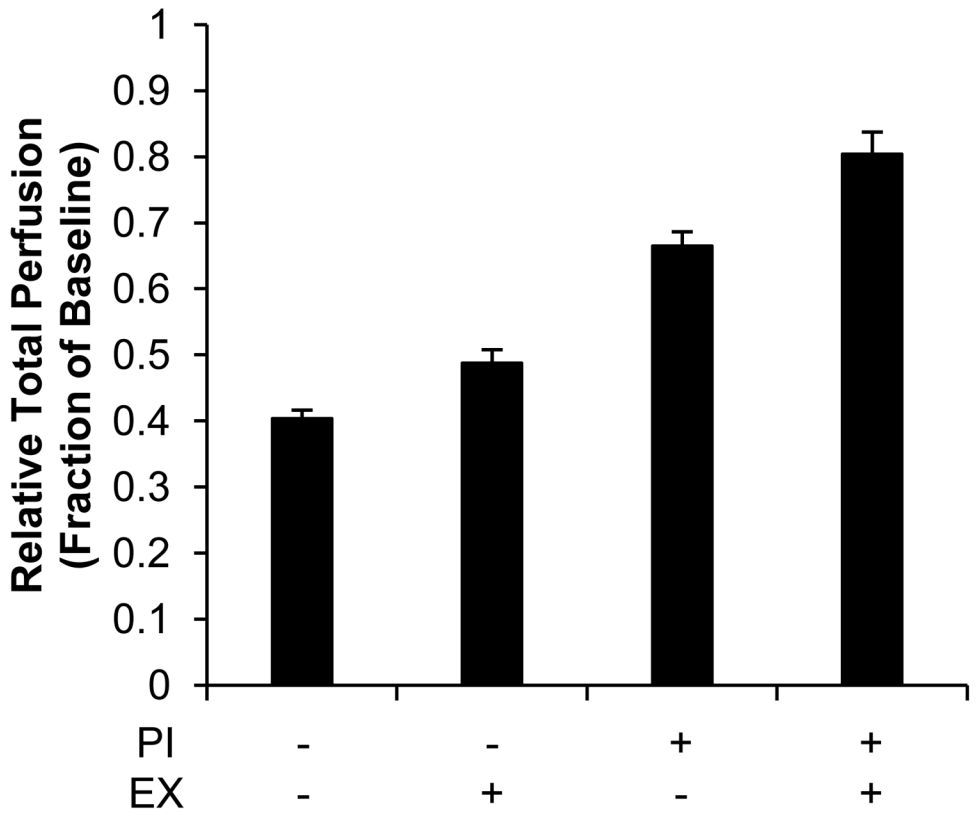

Figure 5. Predicting the relative influence of PAD, exercise, and/or percutaneous intervention on perfusion

Whole muscle network simulations were adapted to reflect PAD conditions (44% rarefaction with 0.6 normalized input pressure). Exercise (EX) was simulated by reducing the degree of rarefaction from 44% to 22%. Percutaneous interventions (PI) were simulated by an increase of normalized input pressure from 0.6 to 0.9. Data are mean ± standard deviation.

Table 1

Microcirculation morphological measurements of the male Sprague-Dawley rat gastrocnemius used for the computational network model construction of an arteriolar tree.

Order	2A	3A	4A	5A	6A	7A
Diameter(μm)	40	28	18	14	10	9
Length(μm)	3200	1800	600	300	250	100
Number	1	2	9	36	80	136